Developmental Cell
Article

Spatial Coordination of Actin Polymerization and ILK–Akt2 Activity during Endothelial Cell Migration

Yi Fan,[1,2] Yanqing Gong,[3] Prabar K. Ghosh,[1] Linda M. Graham,[4] and Paul L. Fox[1,2,*]
[1]Department of Cell Biology, Lerner Research Institute, Cleveland Clinic, 9500 Euclid Avenue, Cleveland, OH 44195, USA
[2]Department of Pathology, Case Western Reserve University, 10900 Euclid Avenue, Cleveland, OH 44106, USA
[3]Department of Molecular Cardiology
[4]Department of Biomedical Engineering
Lerner Research Institute, Cleveland Clinic, 9500 Euclid Avenue, Cleveland, OH 44195, USA
*Correspondence: foxp@ccf.org
DOI 10.1016/j.devcel.2009.03.009

SUMMARY

Eukaryotic cell migration proceeds by cycles of protrusion, adhesion, and contraction, regulated by actin polymerization, focal adhesion assembly, and matrix degradation. However, mechanisms coordinating these processes remain largely unknown. Here, we show that local regulation of thymosin-β4 (Tβ4) binding to actin monomer (G-actin) coordinates actin polymerization with metalloproteinase synthesis to promote endothelial cell motility. In particular and quite unexpectedly, FRET analysis reveals diminished interaction between Tβ4 and G-actin at the cell leading edge despite their colocalization there. Profilin-dependent dissociation of G-actin–Tβ4 complexes simultaneously liberates actin for filament assembly and facilitates Tβ4 binding to integrin-linked kinase (ILK) in the lamellipodia. Tβ4–ILK complexes then recruit and activate Akt2, resulting in matrix metalloproteinase-2 production. Thus, the actin–Tβ4 complex constitutes a latent coordinating center for cell migratory behavior, allowing profilin to initiate a cascade of events at the leading edge that couples actin polymerization to matrix degradation.

INTRODUCTION

Adherent cell locomotion is a highly integrated process, initiated by forward extension of lamellipodia, and proceeding by repeated cycles of protrusion, adhesion, and contraction (Lauffenburger and Horwitz, 1996; Pollard and Borisy, 2003). The individual cellular processes in turn require orchestration of events at the molecular level; e.g., lamellipodial extension demands precise coordination of actin polymerization, matrix degradation, and assembly/disassembly of focal adhesions. Thymosin β4 (Tβ4) is a candidate regulator of cell protrusion because it is a multifunctional, "moonlighting" protein with important roles in distinct protrusion-related processes: actin polymerization and matrix metalloproteinase (MMP) expression. Interestingly, Tβ4 has apparently opposing roles in these processes. As the major sequestering protein of monomeric, globular actin (G-actin), Tβ4 is considered to have an antimigratory function because it inhibits actin polymerization in vitro and in vivo and induces cytoskeletal disorganization (Safer et al., 1991; Sanders et al., 1992). In contrast, activation of integrin-linked kinase (ILK) and Akt by Tβ4 is considered promigratory, because these signals induce MMP synthesis (Bock-Marquette et al., 2004). Consistent with the latter findings, overexpression of Tβ4, or treatment with Tβ4 peptide, promotes cell survival, migration, and angiogenesis (Cha et al., 2003; Bock-Marquette et al., 2004; Malinda et al., 1997; Smart et al., 2007). The magnitude of these opposing activities of Tβ4 may provide a critical determinant of cell migration, but the integration of signals and coordination of activities has not been resolved.

Tβ4 sequesters G-actin, rendering it unavailable for actin filament (F-actin) generation (Goldstein et al., 2005). Polarized elongation of F-actin in lamellipodia of migrating cells is well established and is subject to spatial and temporal coordination by multiple signaling molecules, e.g., rho GTPases and PI-3 kinase/Akt, and by actin-binding proteins, e.g., Arp2/3 and cofilin (Lauffenburger and Horwitz, 1996; Ridley et al., 2003). Although G-actin availability is rate-determining for F-actin elongation, little is known about its spatial regulation during cell movement. Passive diffusion into the lamellipodia may provide sufficient G-actin for filament formation (Pollard et al., 2000). However, preferential G-actin accumulation in protruding zones of the leading edge of migrating cells suggests the possibility of active G-actin polarization during migration (Cao et al., 1993).

In addition to its intracellular actin-sequestering activity, extracellular administration of Tβ4 induces MMP expression in several cell types, including endothelial cells (EC) (Cierniewski et al., 2007; Philp et al., 2006; Qiu et al., 2007). MMP-mediated matrix degradation at the cell surface, particularly at the leading edge, is essential for migration of adherent cells. MMP-2 and membrane-type MMPs are critical for EC migration and for the angiogenic switch to an invasive phenotype (Haas and Madri, 1999; Malik and Kakar, 2006). The mechanism by which Tβ4 stimulates MMP expression is unclear, but it may be mediated by ILK (Bock-Marquette et al., 2004). The interaction of Tβ4 with ILK activates Akt, which promotes cell migration and survival. Moreover, ILK expression is upregulated by Tβ4, and ILK induces MMP-2 expression in epithelial cells and increases cell movement during the epithelial-to-mesenchymal transition (Li et al., 2003; Huang et al., 2007).

Profilin (PFN) is a potential mediator of Tβ4-mediated migration events, because it releases G-actin from Tβ4 and facilitates actin polymerization (Pantaloni and Carlier, 1993). In addition, PFN interacts with multiple promigratory proteins, including Rac/Rho, ROCK, and proline-rich vasodilator-stimulated phosphoprotein (VASP), exhibiting characteristics of a protein interaction platform that facilitates convergence of these signals (Witke, 2004). Preferential localization of PFN at the protrusive edge in fibroblasts (Buss et al., 1992) suggests PFN regulates local signal activation events and actin dynamics during cell migration, consistent with a role for PFN in modulating the potential effects of Tβ4 on G-actin availability and metalloproteinase synthesis.

Here, we show that the interaction between Tβ4 and G-actin is polarized, with diminished interaction at the leading edge of migrating EC. Polarized dissociation of the actin–Tβ4 complex increases the flux of actin from the Tβ4-bound form to the F-actin pool and actin polymerization at the leading edge. Moreover, polarized release of Tβ4 in the cell front permits Tβ4 binding to lamellipodial ILK to facilitate Akt2-ILK interaction and Akt2 phosphorylation, inducing MMP-2 expression. Finally, PFN is required for that polarization and consequent actin polymerization and protease synthesis. These findings establish a mechanism by which spatially restricted release of G-actin coordinates Tβ4 functions to enhance polarized actin filament formation and metalloproteinase synthesis during EC migration.

RESULTS

Interaction between G-Actin and Tβ4 Is Polarized in Migrating EC

G-actin availability in protrusive lamellipodia is rate limiting for actin filament formation; however, little is known about its spatial distribution during cell movement. G-actin accumulated preferentially at the leading edge of EC induced to migrate by wound injury (Figure 1A), consistent with its appearance in lamellipodial extensions during cell spreading (Cao et al., 1993). Because G-actin available for filament formation depends on local concentration and on the absence of inhibitory binding partners, we examined the distribution of Tβ4, an abundant cytoplasmic protein that sequesters G-actin. Tβ4 (but not Tβ10 used as a control) colocalized with G-actin at the cell leading edge. This result was unexpected because it suggests low availability of G-actin for filament formation. Colocalization does not necessarily indicate physical association, and therefore Förster resonance energy transfer (FRET) was used to examine the spatial distribution of actin–Tβ4 complex in migrating EC. FRET was detected by acceptor photobleaching using enhanced green fluorescent protein (GFP)-actin as donor and *Discosoma sp.* red fluorescent protein (DsRed)-Tβ4 as acceptor. To restrict analysis to monomeric G-actin, cells were transfected with a construct expressing GFP-actin containing a G13R mutation in the nucleotide-binding pocket that prevents polymerization and filament formation in cells (Posern et al., 2002). Fusion protein interaction was confirmed by coimmunoprecipitation (see Figure S1A available online). DsRed-Tβ4 was photobleached near the center or the lamellipodia of migrating EC, and the interaction between Tβ4 and actin^{G13R} was determined as FRET (E_{FRET}) efficiency to GFP-actin^{G13R}. FRET was optimized with Tβ4 fusion proteins with varying linker lengths, and a maximum E_{FRET} of 23% was detected using DsRed-GPVAT-Tβ4 (Figure S1B). E_{FRET} between Tβ4 and actin^{G13R} in the lamellipodia of migrating cells was about 10%, less than half of that observed near the cell center (Figure 1B, left). In quiescent cells, E_{FRET} was similar in the edge and near the center, and both were comparable to that in the center of rapidly migrating cells. Similar results were obtained in EC expressing a different nonpolymerizable actin mutant (actin^{R62D}, data not shown). In a positive control experiment, an E_{FRET} of 34% was detected in EC transfected with pGFP-DsRed with an intrinsic short linker; in a negative control, an E_{FRET} of <3% was detected in EC cotransfected with pDsRed and pGFP (Figure 1B, right).

To more precisely locate the actin–Tβ4 interaction, the spatial distribution of E_{FRET} was measured by sensitized-emission FRET, which depends on simultaneous detection of decreased GFP emission and increased DsRed emission. The results verified the polarized interaction with a low E_{FRET} of about 3% in the lamellipodia of migrating cells despite colocalization of actin^{G13R}-GFP and DsRed-Tβ4 in this region (Figure 1C, top panels). An E_{FRET} of up to 25% was observed in the cell body. In control experiments, cotransfection of migrating EC with plasmids expressing GFP and DsRed showed uniformly weak interaction throughout the cell ($E_{FRET} \approx 4\%$), and transfection with GFP-DsRed-expressing plasmid exhibited high-level FRET ($E_{FRET} \approx 27\%$) interaction. In addition, actin^{G13R}-GFP accumulated at the leading edge of migrating EC (Figure 1C), confirming G-actin localization detected with DNase I. This confirmation is important because DNase I also binds pointed ends of actin filaments. However, specificity for G-actin is enhanced in the leading edge by capping of F-actin by gelsolin, actinin, and Arp2/3 that prevents DNase I binding. Taken together, these results show that despite colocalization of G-actin and Tβ4 in migrating cells, their interaction is polarized, such that a large amount of the G-actin in lamellipodia is free of Tβ4.

Polarized Dissociation of Actin–Tβ4 Complex Facilitates Actin Polymerization and Cell Motility

We examined whether reduction of Tβ4 expression by a short-hairpin RNA (shRNA) increases G-actin availability and facilitates actin polymerization in migrating cells. ECs were transfected with a bicistronic vector expressing Tβ4 shRNA, and separately expressing GFP for detection of transfected cells. Tβ4 expression was reduced by about 60% and 90% in transiently and stably transfected EC, respectively (Figure 2A). shRNA specificity was shown by the lack of inhibition of Tβ10 expression (Figure 2A). Transient knockdown of Tβ4 using the shRNA increased the amount of G-actin and F-actin in lamellipodia of migrating EC compared to control cells transfected with shRNA targeted to luciferase (Figure 2B). This partial knockdown also increased wound-induced EC migration by about 30 to 40% compared to controls, consistent with the observed increase in available G-actin and F-actin in the cell front (Figure 2C; Movie S1).

The influence of Tβ4 on G-actin availability and cell migration was investigated further in cells overexpressing actin with point mutations at Tβ4-binding sites. Lys11 and Leu17 in Tβ4 are critical for binding to actin (Van Troys et al., 1996) via interaction with cognate actin sites Glu167 and Asp24 (Irobi et al., 2004; Safer et al., 1997). His-tagged, actin mutants containing D24A,

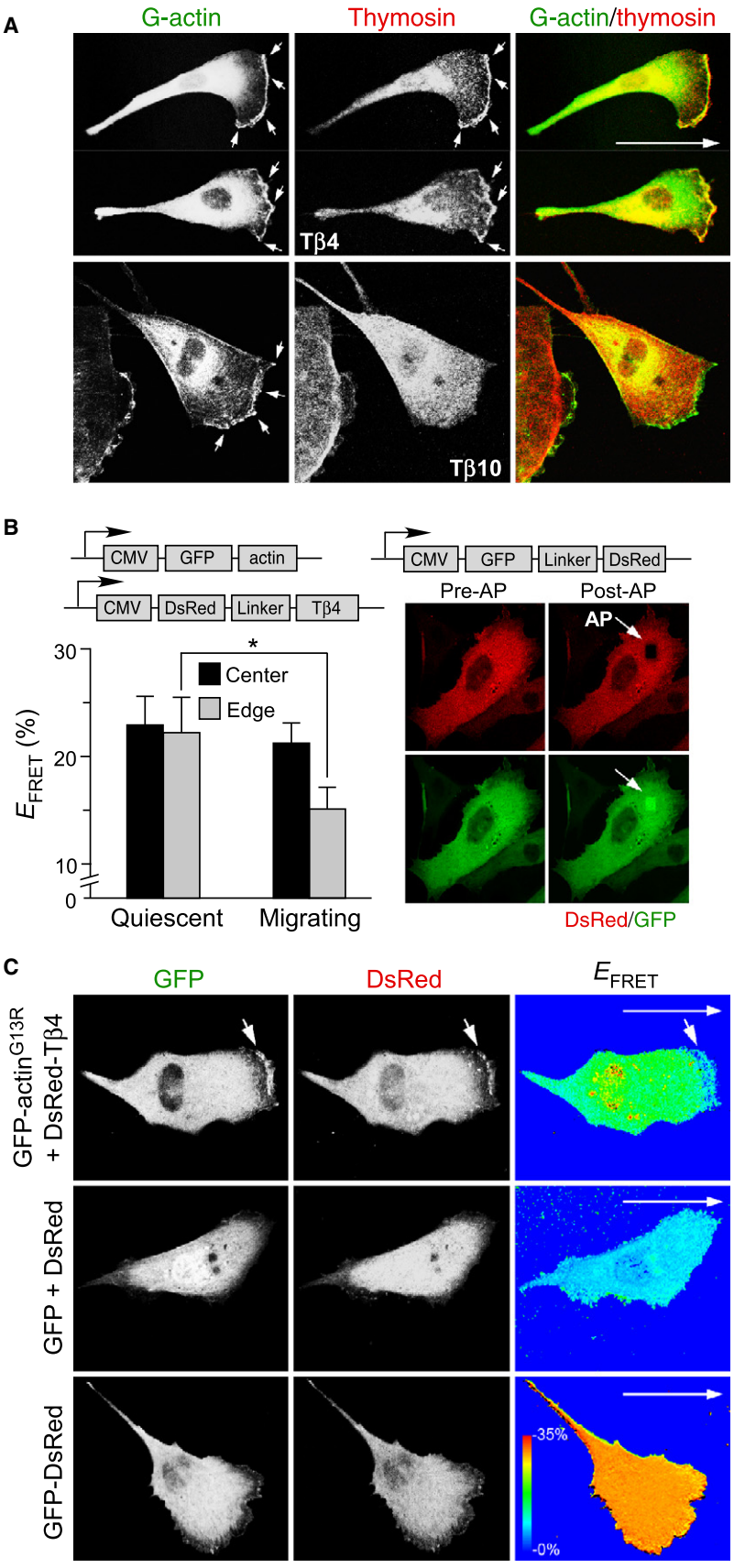

Figure 1. Polarized Interaction between G-Actin and Tβ4 in EC Subjected to Wound-Induced Migration

(A) Preferential localization of G-actin and Tβ4 at the leading edge. G-actin and F-actin were visualized by immunofluorescence using Alexa Fluor 488-conjugated DNase I and Alexa 350-phalloidin, respectively. Tβ4 or Tβ10 was antibody-treated and visualized with Alexa 568-IgG. Direction of cell migration is shown.

(B) Subcellular interaction between actin^{G13R} and Tβ4 by acceptor photobleaching (AP) FRET. ECs were transfected with pGFP-actin^{G13R} plus pDsRed-Tβ4 (left) or pGFP-DsRed (right, positive control). Cells were fixed and subjected to FRET assay. FRET efficiency (E_{FRET}) in center and edge is shown (mean ± SEM, 8–12 cells).

(C) Distribution of actin^{G13R}–Tβ4 interaction in migrating ECs by sensitized-emission FRET. ECs were transfected with pGFP-actin^{G13R} plus pDsRed-Tβ4, pGFP plus pDsRed (negative control), or pGFP-DsRed (positive control), and E_{FRET} analyzed with PFRET software (n = 6–10 cells).

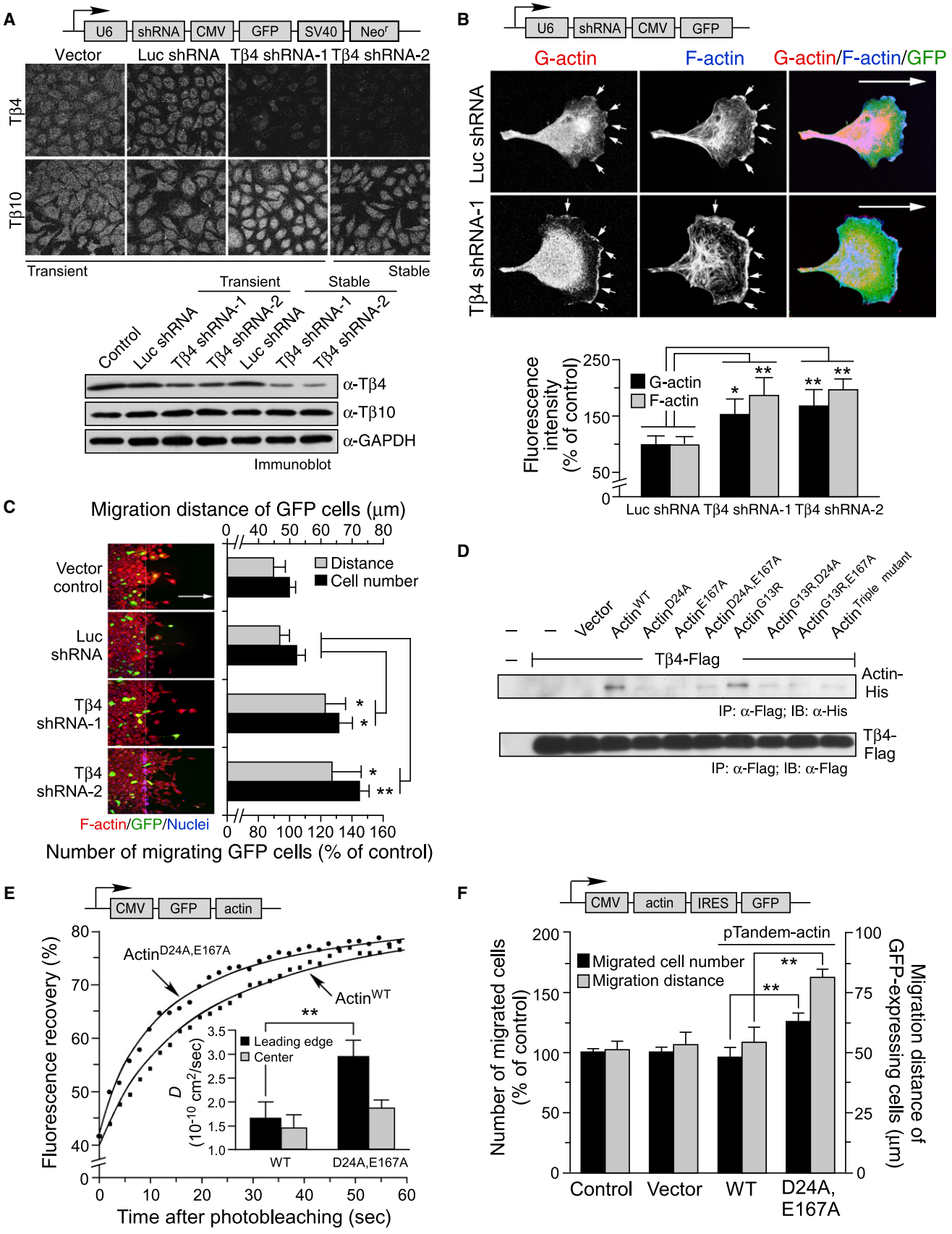
A
U6
shRNA
CMV
GFP
SV40
Neor
Vector
Luc shRNA
Tβ4 shRNA-1
Tβ4 shRNA-2
Tβ4
Tβ10
Transient
Stable
Control
α-Tβ4
α-Tβ10
α-GAPDH
Immunoblot
B
G-actin
F-actin
G-actin/F-actin/GFP
Luc shRNA
Tβ4 shRNA-1
Fluorescence intensity (% of control)
C
Migration distance of GFP cells (μm)
Distance
Cell number
Vector control
Luc shRNA
Tβ4 shRNA-1
Tβ4 shRNA-2
F-actin/GFP/Nuclei
Number of migrating GFP cells (% of control)
D
Tβ4-Flag
Actin-His
IP: α-Flag; IB: α-His
IP: α-Flag; IB: α-Flag
E
CMV
GFP
actin
Fluorescence recovery (%)
Time after photobleaching (sec)
Leading edge
Center
WT
D24A,E167A
F
CMV
actin
IRES
GFP
pTandem-actin
Migrated cell number
Migration distance
Number of migrated cells (% of control)
Migration distance of GFP-expressing cells (μm)
Control
Vector
WT
D24A, E167A

E167A, or both, were coexpressed with Flag-tagged Tβ4. Substantially less Tβ4 bound actin containing either single or double mutations (Figure 2D). The E167A mutation but not D24A slightly suppressed actin binding to profilin-1, and neither affected the interaction with cofilin (Figure S2A). We examined the influence of reduced interaction with Tβ4 on intracellular dynamics of actin during cell migration. Actin polymerization was determined by fluorescence recovery after photobleaching (FRAP). The calculated lateral diffusion coefficient (*D*) of actin-GFP reflects the actin polymerization rate in vivo, not the diffusion rate of actin monomer (McDonald et al., 2006; McGrath et al., 1998; Vasanji et al., 2004). Actin^{D24A,E167A} exhibited an enhanced polymerization rate compared to wild-type as indicated by a 1.6-fold increase in *D* at leading edge; there was no difference in the central area of the cell (Figure 2E). The influence of actin mutants on cell migration was measured in cells transfected with a biscistronic vector expressing GFP. Overexpression of actin carrying single mutation D24A and E167A, or both, markedly enhanced wound-induced cell migration, as measured by the number of migrating cells and by migration distance (Figure 2F and Figures S2B and S2C). In control experiments, normal polymerization of the actin mutants was shown by the filamentous morphology of actin^{D24A,E167A}-GFP chimeras, and overexpression of the fusion proteins did not alter Tβ4 localization (Figure S3). Together, these data indicate that G-actin availability, mediated by polarized dissociation of the actin–Tβ4 complex, is likewise polarized, facilitating actin polymerization at the cell leading edge and enhancing cell migration.

Dissociation of the Actin–Tβ4 Complex Increases MMP-2 Expression and Cell Motility

Polarized dissociation of the actin–Tβ4 complex may influence other Tβ4-mediated migratory events including metalloproteinase synthesis, necessary for extracellular matrix degradation and cell migration (Goldstein et al., 2005). The specific function of Tβ4 was shown in EC stably transfected with shRNA targeted against Tβ4 which markedly reduced MMP-2 activity as measured by gelatin zymography (Figure 3A, top) and confirmed by immunoblot (Figure 3A, bottom). Transfection of cells with human Tβ4 cDNA increased intracellular Tβ4 by about 30% and MMP-2 by about 50% (Figure 3B). Transfection with Tβ4 mutant K11P but not L17A further stimulated MMP-2 synthesis; both mutants bind actin with reduced affinity (Van Troys et al., 1996). The activity of Tβ4 was further tested by a rescue experiment. Transfection of cells with cDNA encoding wild-type or mutant human Tβ4 effectively restored Tβ4 expression in bovine EC stably expressing Tβ4 shRNA-1; the presence of two mismatched nucleotides between human and bovine Tβ4 likely contributed to the bypass of shRNA inhibition. MMP-2 synthesis was partially restored by overexpression of wild-type Tβ4 but completely restored by the K11P mutant, indicating that the actin–Tβ4 interaction is inhibitory (Figure 3B). The L17A mutation did not restore MMP-2 expression, suggesting that an intact LKKTET domain is required for Tβ4-mediated protease synthesis, consistent with the reported role of this domain in Tβ4-induced EC migration and angiogenesis (Philp et al., 2003, 2006).

To evaluate the influence of Tβ4 on cell migration, confluent EC stably expressing shRNA targeted against Tβ4 were induced to migrate by razor wound. Near-complete Tβ4 depletion inhibited cell migration by about 70% (Figure 3C; note that levels of Tβ4 in these experiments are much lower than those in Figure 2C). Overexpression of Tβ4, and especially Tβ4^{K11P}, partially restored migration. The influence of Tβ4 on in vitro angiogenesis was investigated by tube formation in matrigel, a process dependent on both matrix degradation and cell motility. Overexpression of Tβ4 promoted tube formation, and again the Tβ4^{K11P} mutant exhibited greater stimulatory activity (Figure 3D, top). Measurement of cell migration by razor wound gave essentially identical results (Figure 3D, bottom). Taken together, these data reveal a stimulatory role of Tβ4 on MMP-2 synthesis and EC migration. The apparent contradiction with the stimulatory effect of Tβ4 partial knockdown on migration (Figure 2C) suggests a complex relationship between Tβ4 level and cell migration. Possibly, antimigratory sequestration of G-actin and promigratory stimulation of MMP-2 expression exhibit dissimilar dependences on Tβ4 concentration or temporal expression (see below).

Dissociation of the Actin–Tβ4 Complex Promotes Interaction of Tβ4 with ILK and Akt2 Phosphorylation

An interaction between Tβ4 and ILK has been proposed as a promoter of cell migration (Bock-Marquette et al., 2004). Thus, dissociation of the actin–Tβ4 complex may promote an interaction between newly available Tβ4 and ILK to increase MMP-2 expression and cell motility. To test this hypothesis, the interaction of Tβ4 with ILK in the presence or absence of G-actin was determined in vitro by surface plasmon resonance

Figure 2. G-Actin Dissociation from Tβ4 Complex Facilitates Polarized Actin Polymerization and EC Migration

(A–C) Tβ4 knockdown increases G-actin availability, actin polymerization, and EC motility. ECs were transfected with pRANT vectors encoding shRNA targeting luciferase or Tβ4 (#1 or #2). After 96 hr, cells were used for transient transfection or selected to generate stable colonies with 500 μg/ml neomycin.

(A) Tβ4 and Tβ10 expression in transiently or stably transfected ECs was detected by immunofluorescence (top) and immunoblot (bottom).

(B) Increased lamellipodial G-actin and F-actin in Tβ4-knockdown ECs. ECs were transiently transfected with pRNAT vectors and subjected to wound-induced migration. F-actin and G-actin were stained in migrating ECs. Mean fluorescence intensity at the leading edge was quantified with ImagePro software (n = 12–15 cells).

(C) Migration of ECs transiently transfected with pRNAT. Cell migration was determined as number of GFP-expressing ECs that crossed the razor-wound line or by the linear migration distance from the line (mean ± SEM, three experiments).

(D–F) Actin mutation at its Tβ4-binding site increases actin polymerization at the leading edge and EC motility.

(D) Actin mutations of D24A and E167A disturb Tβ4–actin interaction. ECs were cotransfected with pcDNA-Tβ4-FLAG plus EV or pTandem-actin-His. Tβ4 was immunoprecipitated with anti-FLAG antibody, and bound actin-His identified by immunoblot.

(E) Actin polymerization was determined by FRAP at the leading edge and center of migrating ECs overexpressing actin^{WT} or actin$^{D24A+E167A}$. Representative fluorescence recovery curves at the leading edge are shown. Inset: calculated lateral diffusion coefficients, *D* (mean ± SEM, n = 10–12 cells).

(F) Migration ECs overexpressing WT or mutant actin. Number and mean distance of migrating GFP-positive ECs were expressed as percentage of no-transfection controls (mean ± SEM, three experiments).

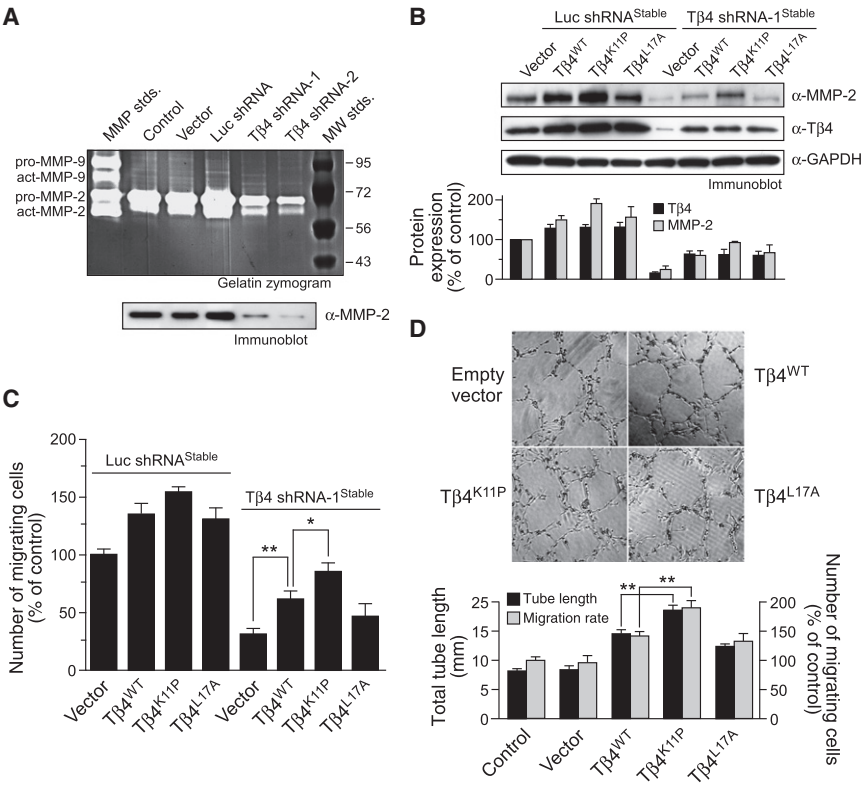

Figure 3. Uncoupling Tβ4–Actin Interaction Increases MMP-2 Expression and Cell Motility

(A) MMP-2 is a major Tβ4-responsive protease in migrating ECs. Protease activity and MMP-2 protein level were detected by gelatin zymography and immunoblot analysis of conditioned medium from subconfluent, migrating ECs stably expressing Tβ4 shRNA-1, -2, or control shRNAs.

(B and C) Actin mutation at Tβ4-binding site, K11P, enhances Tβ4 restoration of MMP-2 expression and cell motility in Tβ4-depleted ECs. ECs stably expressing Tβ4 or Luc shRNA were transfected with pcDNA (vector), pcDNA-Tβ4^{WT}, pcDNA-Tβ4^{K11P}, or pcDNA-Tβ4^{L17A}. MMP-2 and Tβ4 were quantitated densitometrically (three experiments).

(B) MMP-2 secretion by subconfluent migrating EC. Tβ4 and GAPDH in cell lysates were analyzed by immunoblot, and band intensity of Tβ4 was quantified with NIH ImageJ software (mean ± SEM, three experiments).

(C) Transfected cells were subjected to wound-induced migration (mean ± SEM, three experiments).

(D) K11P mutation increases Tβ4-induced EC migration and angiogenesis. ECs were transfected with pcDNA (vector), pcDNA-Tβ4^{WT}, pcDNA-Tβ4^{K11P}, or pcDNA-Tβ4^{L17A} and subjected to wound-induced migration or in vitro angiogenesis analysis using Matrigel. Representative images and calculated total tube lengths are shown (mean ± SEM, three experiments).

(SPR). Chimeric ILK-myc/His expressed in insect cells bound with moderate affinity (Kd = 18.7 μM) to Tβ4 immobilized on the sensor chip (Figure 4A). Less tight interaction was observed for bacterially expressed GST-ILK (Kd > 0.2 mM), suggesting that a high-affinity interaction may require a posttranslational modification. We investigated whether Tβ4 binds at or near the ILK kinase domain (ILK-KD). Tβ4 binding to immobilized GST-ILK-KD was shown by SPR (Figure 4B). Preincubation of Tβ4 with G-actin markedly suppressed its interaction with ILK-KD, suggesting that it successfully competes with ILK-KD for Tβ4 binding; indeed, G-actin binds Tβ4 (Kd = 0.7 μM [Yu et al., 1993]) with a higher affinity than the ILK–Tβ4 interaction. In a control SPR experiment, G-actin did not inhibit ILK-KD binding to Tβ4^{K11P}-His or Tβ4^{L17A}-His (Figure 4C), indicating that G-actin binding to Tβ4, not to ILK-KD, inhibits the Tβ4 and ILK-KD interaction (Figure 4B).

We determined whether the interaction of Tβ4 with ILK subsequently affects its interaction with Akt1/2, as both may be kinase targets of ILK. SPR experiments showed that Akt2 (Figure 4D) and Akt1 (data not shown) interact with GST-ILK-KD. Addition of Tβ4 stimulated Akt2 interaction with GST-ILK-KD, primarily by increasing the binding "on-rate." However, Tβ4 (at 10 μM) did not increase Akt1 binding to GST-ILK-KD (data not shown), indicating highly selective stimulation. Furthermore, direct interaction between Tβ4 and Akt2 was not observed (data not shown), suggesting that Tβ4 binding to ILK facilitates Akt2 recruitment to an ILK-KD–Tβ4 complex.

We investigated the influence of Tβ4 and ILK on Akt2 phosphorylation at Ser474, a reported ILK target (Troussard et al., 2003). GST-Akt2 (dephosphorylated) was incubated in vitro with preactivated ILK-myc/His, and Akt2 phosphorylation at Ser474 was detected by immunoblot with anti-phospho-Akt antibody. ILK by itself induced low-level phosphorylation of GST-Akt2 (Figure 4E). Tβ4 substantially increased ILK-mediated Akt2 phosphorylation, and G-actin prevented this increase. Maximal phosphorylation of Akt2 was detected at the lowest level of Tβ4, but the on-rate of Tβ4 binding to Akt2 is dose responsive in the SPR assay, likely due to different assay timescales. Preactivation of ILK-myc/His by incubating it with lysate from migrating cells increased Tβ4–ILK-induced Akt2 phosphorylation, suggesting that posttranslational modifications of ILK may be one of several possible mechanisms leading to Akt2 activation; PI(3)K inhibitor LY294002 attenuated the cell lysate-induced Akt2 phosphorylation, indicating a role in ILK activation (Figure S4). Together, these data suggest that the Tβ4 interaction with ILK facilitates Akt2 binding to ILK-KD, causing Akt2 phosphorylation. Moreover, G-actin prevents Akt2 activation by blocking the interaction between Tβ4 and ILK.

We determined whether a reduction in Tβ4 binding to G-actin in cells results in a reciprocal increase in Tβ4 binding to ILK and its binding partner, PINCH. Flag-Tβ4 bearing K11P or L17A mutations that prevent its interaction with G-actin were expressed in EC. Both mutations markedly reduced Tβ4 interaction with actin (Figure 4F), confirming previous results (Van Troys et al., 1996). Decreased binding to actin was accompanied by increased binding of Tβ4 to both ILK and PINCH. Immunofluorescence confocal scanning microscopy (at a focal plane near the substratum plasma membrane) revealed nearly uniform

cytoplasmic distribution of ILK and PINCH in quiescent cells, as well as colocalization at apparent focal adhesions. However, ILK, and to a lesser extent PINCH, preferentially accumulates at the forward edge of migrating EC, indicating colocalization with actin-free Tβ4 and thus an opportunity for interaction in the lamellipodia (Figure 4G). In control experiments, we found that knockdown of Tβ4, or overexpression of wild-type or mutant Tβ4, did not alter ILK localization in migrating cells (Figures S5–S7).

ILK-Mediated Activation of Akt2 Is Required for Tβ4-Inducible Expression of MMP-2 and EC Motility

We examined whether the ILK–Akt2 interaction is required for Tβ4-induced metalloproteinase expression and cell migration. Overexpression of Tβ4 substantially increased MMP-2 expression (Figure 5A). The induction was inhibited by PI(3)K inhibitors wortmannin and LY294002 (Figure 5A) and by siRNA-mediated knockdown of Akt2 (Figure 5B), indicating a specific requirement for Akt2 activity. Knockdown of ILK likewise suppressed Tβ4-induced MMP-2 expression (Figure 5C). Tβ4 markedly increased phosphorylation of Akt2 at Ser474 in an ILK-dependent manner; only low-level induction of Akt1 phosphorylation at Ser473 was observed, indicating target specificity (Figure 5D). Finally, Akt2 knockdown inhibited both wound-induced cell migration and chemotaxis (Figure 5E). Together, these data show that productive interaction between ILK and Akt2 is required for Tβ4-induced MMP-2 synthesis and EC migration.

We determined whether ILK–Akt2-induced MMP-2 expression depends on mammalian target of rapamycin (mTOR), a major Akt substrate. Tβ4 overexpression moderately increased PKB/Akt-dependent mTOR activation, as determined by phosphorylation at Ser2448 (Figure S8A). mTOR siRNA attenuated Tβ4-induced MMP-2 expression, indicating a partial dependence of Tβ4-inducible MMP-2 expression on mTOR (Figures S8B and S8C). In summary, Tβ4 dissociation from G-actin complex increases formation of a ternary Tβ4–ILK–Akt2 complex, leading to Akt2 phosphorylation, mTOR activation, and consequent MMP-2 expression to promote cell motility.

Overexpression of Tβ4 carrying the K11P mutation at the actin-binding site induced a small increase in Akt2 phosphorylation (Figure S9A), consistent with the increased restoration of MMP-2 expression in Tβ4-depleted cells (Figure 3B) and with the regulatory role of G-actin in Tβ4-inducible Akt2 phosphorylation in vitro (Figure 4D). Despite the increase in actin polymerization and cell motility (Figure 2), transient knockdown of Tβ4 did not affect Akt phosphorylation or MMP-2 expression (Figure S9B). However, stable depletion of Tβ4 inhibited both MMP-2 expression and cell motility (Figure 3). These results suggest differential sensitivity of ILK–Akt activation and MMP-2 induction to decreases in cellular Tβ4 level.

PFN Is Required for Polarized Actin–Tβ4 Complex Dissociation and Actin Polymerization

PFN dissociates G-actin from Tβ4, and freed G-actin, possibly in association with PFN, facilitates actin polymerization (Pantaloni and Carlier, 1993). Thus, PFN could play a significant role in polarized dissociation of the actin–Tβ4 complex in migrating cells. PFN colocalized with G-actin at the leading edge of migrating EC but distributed uniformly in quiescent ECs (data not shown), consistent with the preferential localization at protrusive edges of fibroblasts (Buss et al., 1992). PFN was efficiently knocked down by siRNA targeting PFN-1 or both PFN-1 and PFN-2 (Figure 6A). PFN-1 knockdown depolarized the actin–Tβ4 interaction in migrating EC, as indicated by uniform E_{FRET} in siRNA-treated EC (Figure 6B), suggesting that PFN increases G-actin availability at the leading edge. PFN-1 knockdown cells remained polarized during random cell migration, but the fraction of polarized cells was reduced (Figure S10). Consistent with a previous report (Ding et al., 2006), PFN-1 siRNA did not exhibit compensatory upregulation of PFN-2 (data not shown). The effect of PFN-1 knockdown on actin polymerization was measured in cells transfected with a biscistronic vector coexpressing GFP-actin and shRNA targeting PFN-1. PFN-1 knockdown almost completely blocked formation of lamellipodial F-actin (Figure 6C). These data establish an essential role of PFN-1 in the spatially restricted dissociation of the actin–Tβ4 complex, and consequent polarization of G-actin during cell migration.

PFN Enhances Tβ4–ILK Interaction to Promote MMP-2 Synthesis during Cell Migration

PFN-mediated release of Tβ4 from its complex with G-actin can influence a second promigratory pathway; i.e., it can facilitate the interaction of Tβ4 with ILK and thereby increase metalloprotease synthesis. Indeed, PFN-1 knockdown induced a phenotypic switch characterized by a 70% increase in the actin–Tβ4 interaction and about a 60% decrease in the interaction of Tβ4 with ILK (and with PINCH to a lesser extent) (Figure 7A). The diminished Tβ4–ILK interaction is expected to decrease Akt2 activation, and consequently inhibit MMP-2 expression. In fact, PFN-1 knockdown markedly reduced MMP-2 expression in migrating cells to nearly the level observed in quiescent cells and decreased MMP-2 activity (Figure 7B), consistent with the observed decrease in Akt2 phosphorylation at Ser474 (Figure S10B). The somewhat greater effectiveness of the PFN knockdown (which depletes both PFN-1 and PFN-2) compared to the PFN-1 knockdown suggests a possible role for PFN-2 in Tβ4-induced MMP-2 synthesis. Overexpression of Tβ4, particularly the actin-blind $Tβ4^{K11P}$ mutant, significantly restored MMP-2 expression in PFN-1 knockdown cells (Figure 7C). PFN knockdown inhibited wound-induced EC migration by about 50% to 60% (Figure 7D; Figure S10C). Migration was partially rescued by co-overexpression of $Tβ4^{K11P}$ and $actin^{D24A,E167A}$ but not by either protein by itself (Figure 7E). The incomplete restoration may be due to disrupted activity of other motility-related, PFN-interacting proteins, e.g., Rac/Rho, ROCK, VASP, and WASP, required for actin crosslinking, branching, and bundling (Witke, 2004). Together, these results suggest that PFN activates a dual function, promigratory switch in which the release of Tβ4 from G-actin promotes both actin polymerization and MMP-2 expression.

DISCUSSION

Our results show that dissociation of the actin–Tβ4 complex is spatially restricted to the leading edge of migrating EC. PFN-dependent, polarized dissociation increases the flux of actin from the Tβ4-bound form to the F-actin compartment at the

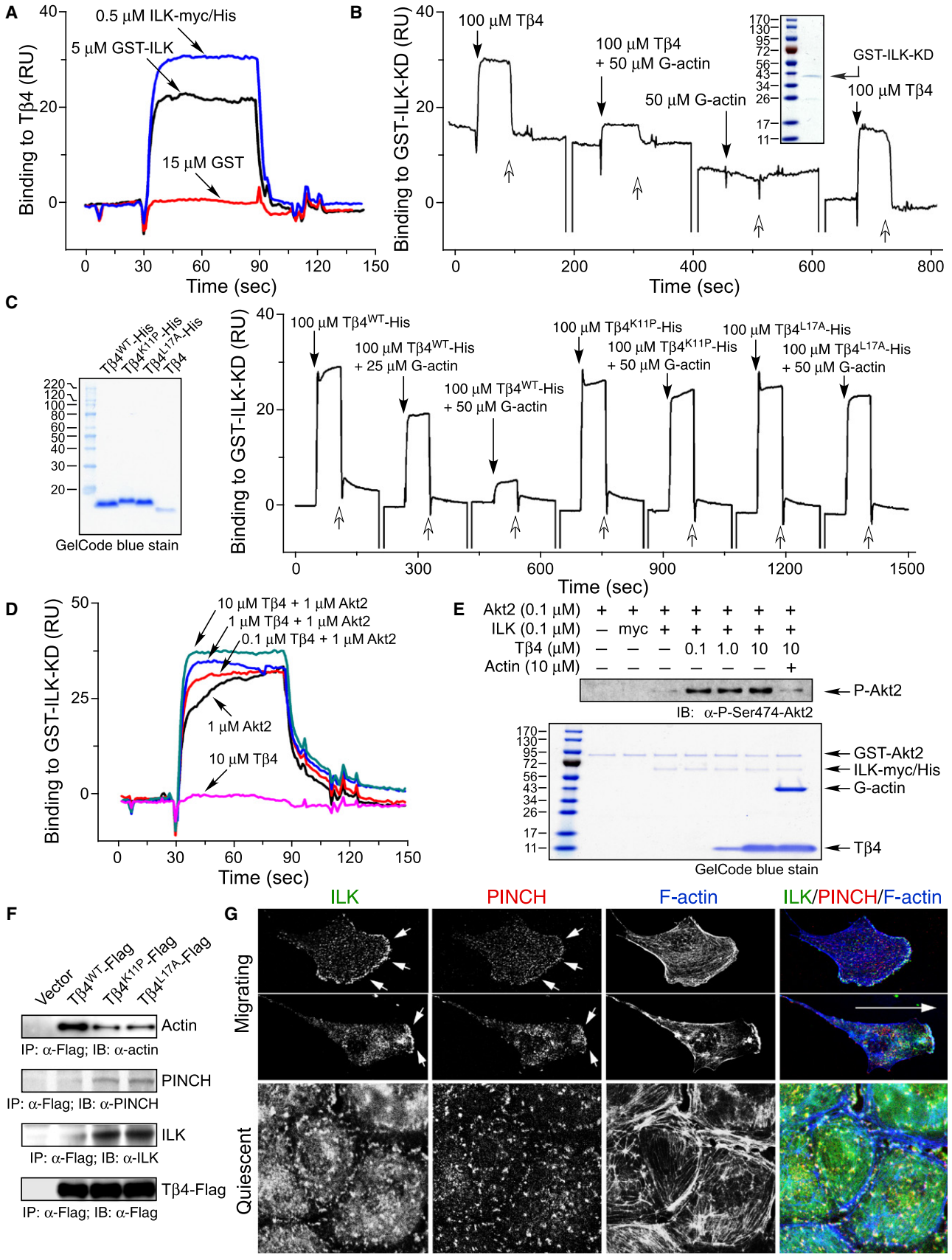
A
0.5 μM ILK-myc/His
5 μM GST-ILK
15 μM GST
Binding to Tβ4 (RU)
Time (sec)
B
100 μM Tβ4
100 μM Tβ4
+ 50 μM G-actin
50 μM G-actin
100 μM Tβ4
GST-ILK-KD
Binding to GST-ILK-KD (RU)
Time (sec)
C
GelCode blue stain
100 μM Tβ4WT-His
100 μM Tβ4WT-His
+ 25 μM G-actin
100 μM Tβ4WT-His
+ 50 μM G-actin
100 μM Tβ4K11P-His
100 μM Tβ4K11P-His
+ 50 μM G-actin
100 μM Tβ4L17A-His
100 μM Tβ4L17A-His
+ 50 μM G-actin
Binding to GST-ILK-KD (RU)
Time (sec)
D
10 μM Tβ4 + 1 μM Akt2
1 μM Tβ4 + 1 μM Akt2
0.1 μM Tβ4 + 1 μM Akt2
1 μM Akt2
10 μM Tβ4
Binding to GST-ILK-KD (RU)
Time (sec)
E
Akt2 (0.1 μM)
ILK (0.1 μM)
Tβ4 (μM)
Actin (10 μM)
P-Akt2
IB: α-P-Ser474-Akt2
GST-Akt2
ILK-myc/His
G-actin
Tβ4
GelCode blue stain
F
Vector
Tβ4WT-Flag
Tβ4K11P-Flag
Tβ4L17A-Flag
Actin
IP: α-Flag; IB: α-actin
PINCH
IP: α-Flag; IB: α-PINCH
ILK
IP: α-Flag; IB: α-ILK
Tβ4-Flag
IP: α-Flag; IB: α-Flag
G
ILK
PINCH
F-actin
ILK/PINCH/F-actin
Migrating
Quiescent

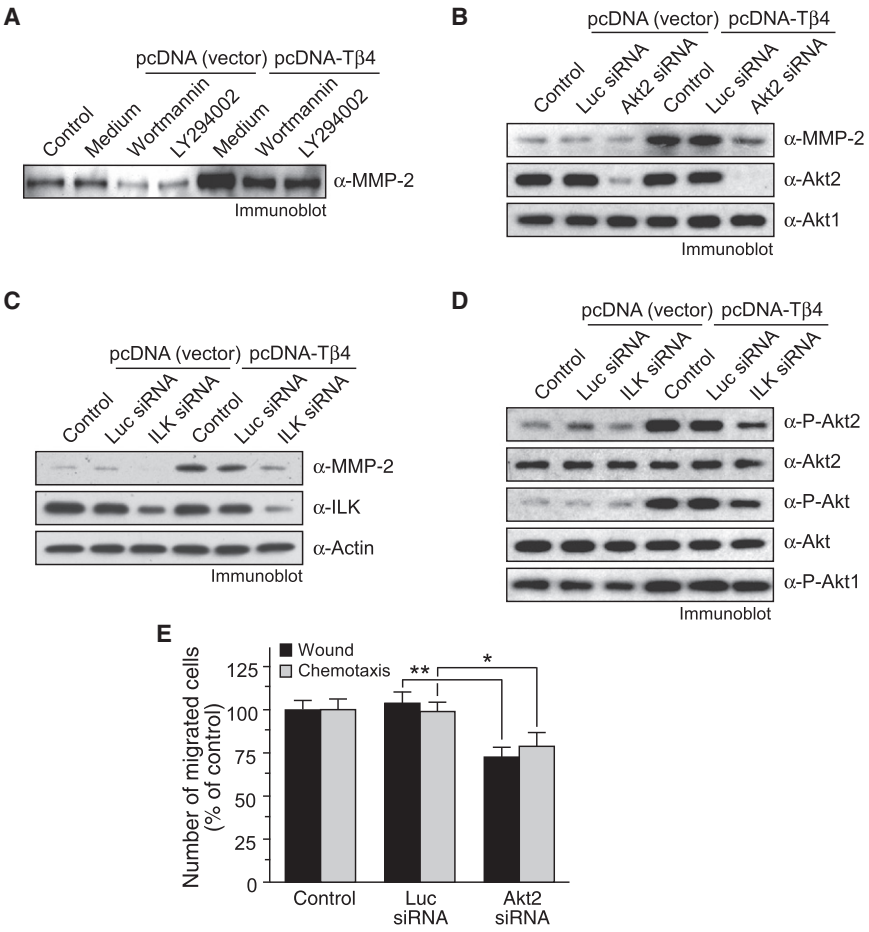

Figure 5. Tβ4-Induced, ILK-Mediated Akt2 Activation Is Required for MMP-2 Expression and EC Motility

(A and B) Tβ4-induced MMP-2 expression requires Akt2. ECs transfected with pcDNA (vector) or pcDNA-Tβ4 were treated with 100 nM wortmannin, 1 μM LY294002, or medium for 2 hr, or Akt2 or Luc siRNA overnight, and allowed to migrate for 8 hr. MMP-2 was detected in the EC-conditioned medium. Intracellular Akt1 and Akt2 were determined by immunoblot.

(C and D) Tβ4-induced Akt2 phosphorylation and MMP-2 expression require ILK. ECs were transfected with pcDNA vector or pcDNA-Tβ4, treated with Luc or ILK siRNA, and allowed to migrate for 8 hr. The secreted MMP-2 was detected in the cell-conditioned medium, and ILK was detected by immunoblot of lysate. Akt phosphorylation was detected with anti-phospho-Akt1-, phospho-Akt2-, or phospho-Akt antibodies, and antibodies against total Akt, Akt2, and GAPDH were used as controls.

(E) Akt2 is required for EC migration. ECs were incubated with or without Luc siRNA or Akt2 siRNA and subjected to wound-induced or chemotactic migration across collagen I-coated transwell with 10% FBS as chemoattractant (mean ± SEM, triplicates).

leading edge. Concurrently, the release of Tβ4 from G-actin facilitates formation of an ILK–Tβ4–Akt ternary complex that increases Akt phosphorylation (Figure 7F). The resultant activation of Akt2 induces MMP-2 synthesis to facilitate matrix degradation, and Akt1 activation promotes actin polymerization at the leading edge.

Polarized Actin-Tβ4 Interaction Spatially Regulates G-Actin Availability and Facilitates Actin Polymerization

Cell locomotion is driven by polarized F-actin growth that is rate determined by the availability, i.e., the time-integrated amount of G-actin available for polymerization, in the leading edge. PFN increases G-actin availability by increasing the flux from the Tβ4–G-actin pool but decreases G-actin concentration by promoting addition to F-actin filaments. The high intracellular ratio of Tβ4:G-actin (e.g., 0.4 mM:0.1 mM in human platelets) suggests that most cytosolic G-actin is sequestered by Tβ4 (Huff et al., 2001; Safer et al., 1991). Our experiments reveal that substantial G-actin is generated at the leading edge by the polarized dissociation of G-actin from Tβ4. The consequences of this interaction were shown by experiments in which the interaction was inhibited by Tβ4 knockdown or by mutation of actin at its Tβ4-binding site. In both cases, we observed increased G-actin availability, lamellipodial polymerization of actin, and cell motility. These results also confirm the important role of regulated

Figure 4. Release of Tβ4 from the Tβ4–G-Actin Complex Enhances Its Interaction with ILK and Akt2 Phosphorylation

(A) Weak interaction between Tβ4 and ILK. Purified, insect cell ILK-myc, bacterial GST-ILK, or GST binding to immobilized Tβ4 on BIAcore chip was determined by SPR.

(B) G-actin blocks Tβ4 binding to kinase domain (KD) of ILK. Tβ4 and G-actin were injected to immobilized ILK-KD. Sensor chip was regenerated between injections. Inset: GelCode blue stain of purified GST-ILK-KD.

(C) Interaction of $Tβ4^{K11P}$ and $Tβ4^{L17A}$ with the ILK kinase domain (ILK-KD) is not inhibited by G-actin. Purified bacterial Tβ4-His fusion proteins (left panel). Purified Tβ4-His fusion proteins containing wild-type (WT) or K11P and L17A mutants were analyzed by SDS-PAGE and stained with GelCode blue; human Tβ4 was used as standard. Effect of G-actin on Tβ4 interaction with ILK-KD (right panel). Wild-type (WT) or mutated Tβ4-His and G-actin solutions were injected and binding to immobilized ILK-KD determined by SPR. Sensor chip regeneration is indicated (open arrows).

(D) Tβ4 increases Akt2 interaction with KD of ILK. Akt2-His binding to the immobilized GST-ILK-KD was detected with or without Tβ4.

(E) Tβ4 increases ILK-induced Akt2 phosphorylation that is inhibited by actin. Purified GST-Akt2 was incubated with preactivated ILK-myc or myc with or without Tβ4 and actin at 30°C for 30 min. Phosphorylation at Ser474 was detected by phosphospecific antibody and total protein by GelCode blue.

(F) Tβ4 mutations at its actin-binding sites increase its interaction with ILK/PINCH in migrating ECs. ECs were transfected with pcDNA-Tβ4-FLAG and subjected to random migration. Cell lysates were immunoprecipitated with anti-FLAG and immunoblotted with anti-FLAG, -actin, -PINCH, and -ILK antibodies.

(G) Enrichment of ILK/PINCH at the leading edge during cell migration. Cells were stained with anti-ILK or anti-PINCH antibody, and F-actin visualized with Alexa 350-phalloidin (n = 8 cells).

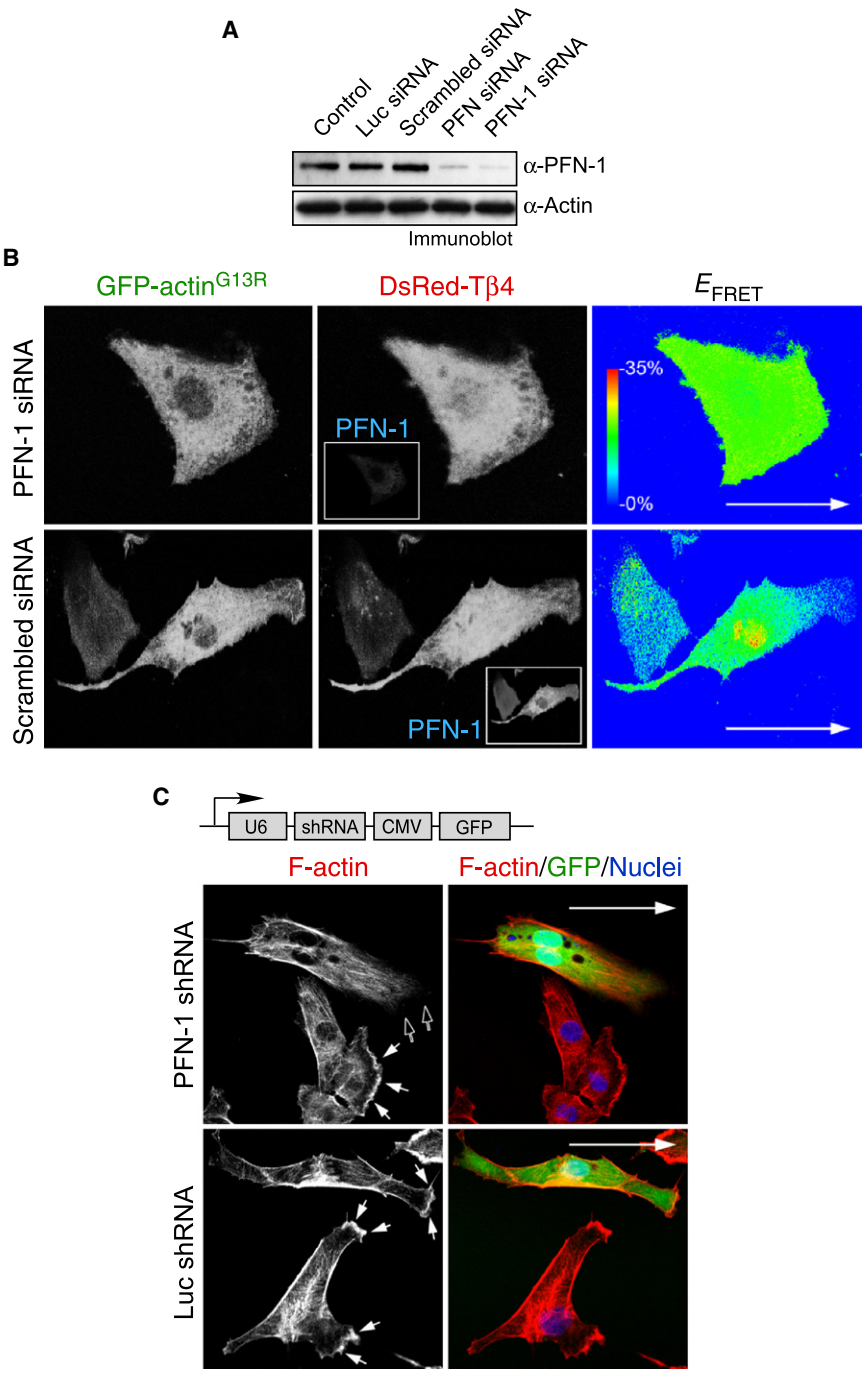

Figure 6. PFN Is Required for Polarization of Tβ4–G-Actin Interaction and Actin Polymerization at the Leading Edge

(A) PFN-1 knockdown. ECs were transfected with siRNA targeting total PFN and PFN-1, or luciferase and scrambled PFN-1 siRNA as controls for 24 hr; 72 hr after transfection, cell lysate was immunobloted with anti-PFN-1 and -actin antibodies.

(B) PFN-1 knockdown abolishes polarization of Tβ4–G-actin interaction. ECs were pretreated with PFN-1 siRNA or control scrambled siRNA, cotransfected with pGFP-actin^{G13R} plus pDsRed-Tβ4, and subjected to wound-induced migration for 24 hr. PFN-1 in fixed cells was detected by immunofluorescence with Alexa 350-IgG, and E_{FRET} between actin^{G13R} and Tβ4 in fixed, migrating cells was analyzed.

(C) PFN-1-knockdown inhibits actin polymerization at the leading edge. Cells were transfected with pRANT-GFP plasmids encoding PFN-1 or Luc shRNA. Migrating cells were fixed and stained for F-actin visualization.

G-actin availability in cell motility. A contrasting result was reported in tumor cells in which Tβ4 knockdown decreased cell migration (Kobayashi et al., 2002). The different response may be due to a greater dependence on Tβ4-inducible protease expression for tumor cell movement in a matrix-rich environment.

Dissociation of Tβ4 from the Actin–Tβ4 Complex Induces ILK–Akt2-Mediated MMP-2 Expression

ILK phosphorylates PKB/Akt (Delcommenne et al., 1998) and binds PINCH, paxillin, and parvin (Wu and Dedhar, 2001), all important components regulating cell migration. ILK is critical for EC migration and angiogenesis (Friedrich et al., 2004; Tan et al., 2004; Vouret-Craviari et al., 2004). The mechanism by which Tβ4 stimulates MMP expression is unclear (Bock-Marquette et al., 2004). Because Tβ4 coimmunoprecipitates with ILK–PINCH, activation of Akt in the ILK–Akt complex could be responsible for MMP expression and increased cell migration. Our studies show an interaction of Tβ4 with the kinase domain of ILK, and that formation of the ternary Tβ4–ILK–Akt2 complex increases Akt2 phosphorylation with a consequent increase in MMP-2 expression and cell migration. These Tβ4-mediated processes are regulated by G-actin binding to Tβ4: dissociation of actin–Tβ4 complex promotes Tβ4–ILK interaction and MMP-2 expression. Thus, these results provide a molecular mechanism for Tβ4-promoted protease synthesis and cell migration.

The Akt family consists of three isoforms: Akt1, Akt2, and Akt3. The role of Akt2 in cell migration is controversial: Akt2 knockout elevates Rac and Pak1 activities to increase fibroblast cell motility (Zhou et al., 2006), but our knockdown studies indicate that Tβ4-inducible Akt2 activation induces protease synthesis to facilitate EC migration. Consistent with our findings, transient knockdown or overexpression studies show a stimulatory role of Akt2 in cell migration and invasion in multiple cell types (Arboleda et al., 2003; Cheng et al., 2007; Irie et al., 2005; Sithanandam et al., 2005). Thus, Akt2 may have dual roles in induction of MMP and inhibition of migratory signaling, including Rac. Akt1 is critical for actin polymerization and cell motility, particularly for EC migration (Ackah et al., 2005; Chen

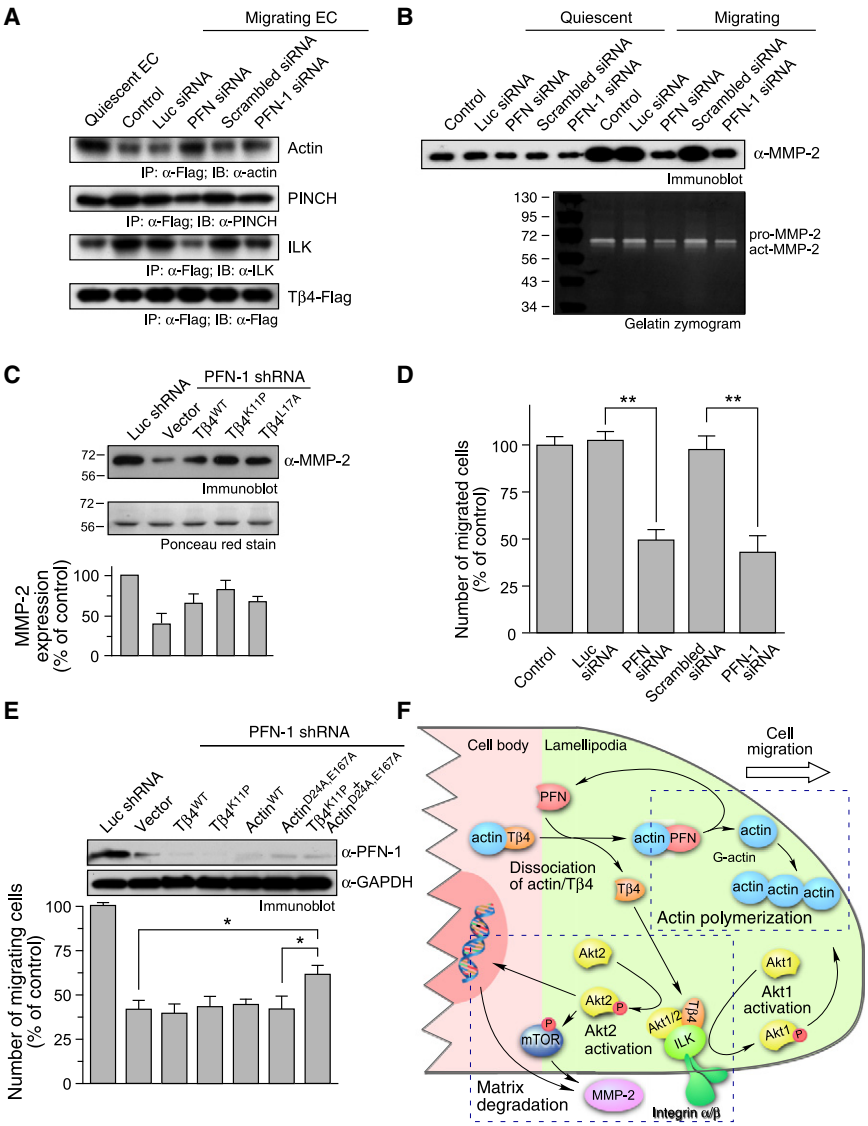

Figure 7. PFN Increases Tβ4–ILK Interaction to Promote MMP-2 Expression

(A) PFN knockdown increases Tβ4–actin binding and attenuates Tβ4 interaction with ILK/PINCH in migrating ECs. ECs were transfected with PFN siRNA or PFN-1 siRNA, or Luc siRNA or scrambled siRNA as controls, for 24 hr, and then transfected with pcDNA-Tβ4-FLAG. Cell lysates from subconfluent, migrating cells and confluent, quiescent cells were immunoprecipitated with anti-FLAG antibody and immunoblotted with anti-actin, -PINCH, -ILK, and -FLAG antibodies.

(B) PFN knockdown inhibits MMP-2 expression and activity during cell migration. ECs were transfected with or without Luc, PFN, scrambled, or PFN-1 siRNA. Secreted MMP-2 was detected in conditioned medium of confluent quiescent or subconfluent migrating cells. MMP-2 protein was determined by immunoblot and metalloproteinase activity by gelatin zymography. Results are representative for three independent assays.

(C) Overexpression of $T\beta4^{K11P}$ restores MMP-2 expression in PFN-1-knockdown cells. Cells were transfected with pRNAT-Luc, or pRNAT-PFN-1 plus pcDNA (vector), or pcDNA-Tβ4 with or without mutations. MMP-2 was detected by immunoblot in conditioned medium of subconfluent migrating cells and quantified with NIH ImageJ software (mean ± SEM, two experiments).

(D) PFN knockdown inhibits EC migration. ECs were treated with siRNAs indidcated and subjected to wound-indudced migration (mean ± SEM, four experiments).

(E) Overexpressin of $T\beta4^{K11P}$ and $actin^{D24A,E167A}$ partially rescues cell migration in PFN-knockdown cells. Cells were transfected with pRNAT-Luc, or pRNAT-PFN-1 plus pcDNA (vector), pcDNA-Tβ4, or pcDNA-actin with or without mutations. Three days after transfection, confluent cells were subjected to wound-induced cell migration (mean cell number ± SEM, two experiments, $^*p < 0.05$). Inset, cell lysates were immunoblotted with anti-PFN-1 and -GAPDH antibodies.

(F) Schematic. Polarized interaction between G-actin and Tβ4 integrates Tβ4's activities to coordinate actin polymerization and matrix degradation during cell migration. PFN induces spatially restricted dissociation of Tβ4-G-actin in lamellipodia, and this polarization generates local G-actin availability to promote polarized actin polymerization, and meanwhile releases actin-free Tβ4 that interacts with preferentially lamellipodia-localized ILK, leading to Akt phosphorylation. Subsequent Akt2 activation induces MMP-2 synthesis followed by ECM degradation, and Akt1 activation locally promotes actin polymerization, both facilitating cell migration.

et al., 2005) and in vivo angiogenesis (Ackah et al., 2005; Phung et al., 2006). Our data show that Tβ4 stimulates stronger ILK-mediated activation of Akt2 than that of Akt1. We speculate that weaker Akt1 induction results in a tighter localization of active Akt1 to the leading edge (data not shown), enhancing local actin polymerization.

There is evidence that ILK is a kinase-inactive "pseudokinase" (Boudeau et al., 2006). However, ILK phosphorylation of Akt1 at Ser473 has been shown (Delcommenne et al., 1998) and recently confirmed (Joshi et al., 2007; White et al., 2006). Our experiments suggest that ILK phosphorylates Akt2 at Ser474, that Akt2 is a better substrate than Akt1, and that a posttranslational modification to ILK is required for its activity. Our results may help to explain the absence of detectable ILK-mediated Akt1 phosphorylation in some conditions.

Polarized Dissociation of Actin–Tβ4 Complex Coordinates Tβ4's Dual Migratory Functions of Actin Polymerization and Protease Synthesis

Cell protrusion requires spatial and temporal coordination of actin polymerization, matrix degradation, and assembly/disassembly of focal adhesions. Several mechanisms may coordinate actin polymerization and cell adhesion during cell migration, including biphasic, fibronectin-dependent Rac activation (Cox et al., 2001), Rho-mediated feedback (Ren et al., 1999), and myosin II-regulated mechanical responses (Giannone et al., 2007; Gupton and Waterman-Storer, 2006). Our results indicate that regulated dissociation of Tβ4–G-actin coordinates motility-related processes: locally released G-actin and Tβ4 induce actin polymerization and ILK–Akt2-mediated MMP-2 synthesis, respectively. The high intracellular ratio of Tβ4-to-G-actin presents an

argument against a regulatory role for actin–Tβ4 complex dissociation since excess free Tβ4 would be expected to bind ILK constitutively. However, we show that alteration of intracellular Tβ4 level by siRNA-mediated silencing or by cDNA overexpression modulates MMP-2 expression and cell motility. These results provide compelling evidence that the amount of *available* Tβ4 is not in excess in nonstimulated cells, and that PFN-mediated release of Tβ4 from G-actin can indeed cause biologically significant downstream consequences. Possibly, the apparent inconsistency is explained by low-affinity binding of excess Tβ4 to F-actin (Ballweber et al., 2002; Carlier et al., 1996), particularly at the leading edge where F-actin is highly enriched. Thus, sequestration of Tβ4 by both actin forms may prevent interaction with ILK in quiescent cells, until specifically released from G-actin at the cell front during migration. Our experiments are consistent with previous reports of exogenous Tβ4 enhancing MMP-2 expression and cell migration (Philp et al., 2006). Moreover, our results suggest that interaction of Tβ4 with cell surface receptors is not necessary for its activity.

Tβ4 binding to G-actin negatively regulates G-actin availability and consequent actin polymerization, whereas Tβ4 binding to ILK enhances Akt2-dependent MMP-2 expression and extracellular matrix degradation. These Tβ4-dependent events have opposing effects on cell migration that results in a complex, multiphasic dependence of motility on intracellular Tβ4 (Figure S11). Our data are consistent with a model in which Tβ4 overexpression results in an increase in MMP-2 expression that more than compensates for decreased G-actin availability, resulting in increased cell movement. Paradoxically, Tβ4 knockdown results in an increase in G-actin availability that more than compensates for decreased MMP-2 expression, again resulting in increased cell movement. However, deep depletion of Tβ4 almost completely suppresses MMP-2 expression and matrix degradation, forming a migration barrier accompanied by cortical F-actin enrichment (data not shown) even in the presence of a high level of available G-actin.

In summary, our results show that PFN induces polarized dissociation of actin–Tβ4 complex resulting in G-actin availability at the leading edge of a motile EC. The spatially restricted dissociation process enhances cell movement by simultaneously promoting actin polymerization and inducing formation of a ternary Tβ4–ILK–Akt2 complex which induces MMP-2 synthesis. These findings provide a new mechanism for coordination of actin polymerization and matrix degradation during cell migration.

EXPERIMENTAL PROCEDURES

Cell Culture and Migration

Bovine ECs isolated from adult bovine aortas were cultured in DME/Ham's F-12 medium (GIBCO, Gaithersburg, MD) containing 5% fetal bovine serum (FBS) at 37°C in a humidified atmosphere of air containing 5% CO_2. Human umbilical vein ECs were maintained in MCDB medium with 10% FBS. EC migration was quantitated by "razor-wound" method (Ghosh et al., 2002).

Plasmids and Transfection

pEGFP-actin and pEGFP-C1 were from Clontech (Mountain View, CA). Wild-type and mutant actin cDNAs were amplified by PCR as KpnI/XhoI fragments and cloned into pcDNA 3.1/*myc*-His (Invitrogen, Carlsbad, CA). GFP cDNA, amplified from pEGFP-C1, was cloned into pTandem-1 (Novagen, San Diego, CA) immediately after the IRES, and actin cDNAs as NcoI/XhoI fragments were cloned into the plasmids before IRES with a polyHis tag. The Tβ4 gene coding region was amplified from a bovine cDNA pool (BioChain, Hayward, CA) and cloned into pDsRed-N1 (gift from Dr. Yang Guo, Cleveland Clinic) with respective linker sequences, or into pcDNA 3.1 with or without FLAG-tag. GFP cDNAs with linker sequences were cloned into pDsRed-N1 to express GFP-DsRed chimeras. All cloned plasmids were verified by enzyme digestion and sequencing. ECs at 40% confluence were transfected with plasmids using lipofectin (Invitrogen) in serum-free Opti-MEM medium (Invitrogen) overnight.

Mutagenesis

Actin and Tβ4 mutants were generated by PCR using GeneTailor Site-Directed Mutagenesis System (Invitrogen). In brief, pEGFP-actin (Clontech, Mountain View, CA) was used as a template to generate G13R, R62D, and L267D mutations for inhibiting actin polymerization, and D24A and E167A for disrupting interaction of actin and Tβ4. pcDNA-Tβ4 (with or without FLAG tag) was used as a template to generate K11P and L17A mutations. All clones were verified by double enzyme digestion and sequencing.

Protein Expression and Purification

ILK cDNA (OriGene, Rockville, MD) was cloned into pcDNA-myc/his as BamHI/XhoI fragment or pET41-GST (Novagen) as NcoI/XhoI fragment. ILK-myc/his was in vitro translated from pcDNA-ILK vector with insect EasyXpress kit (QIAGEN, Valencia, CA) and purified with MagneHis system (Promega). pET-GST-ILK was transformed into Rosetta-gemi2 bacteria (Novagen), and protein expression induced with 0.2 mM IPTG at 30°C for 5 hr with chloramphenicol, streptomycin, tetracycline, and kanamycin. Soluble protein was extracted with CelLytic B cell lysis reagent (Sigma), and GST-ILK was purified with B-PER GST purification kit (Pierce, Rockford, IL). Insect GST-Akt1 and GST-Akt2 were obtained from Cell Signaling Technology, and Akt1-His and Akt2-His from Millipore (Billerica, MA). Tβ4 cDNA was cloned into pTriEx-his (Novagen) as a NcoI/XhoI fragment and expressed in BL21 bacteria by 0.2 mM IPTG induction at 30°C for 3 hr. Tβ4-His was purified using B-PER His purification kit (Pierce).

Surface Plasmon Resonance

Experiments were conducted on BIAcore 3000 instrument (GE Health, Uppsala Sweden) with a running buffer of 10 mM HEPES (pH 7.4), 150 mM NaCl, and 0.005% Surfactant P20 (for high concentration of actin: 5 mM phosphate buffer) at 20 μl/min, 25°C. Purified Tβ4, ILK-myc/his, or ILK-KD was immobilized on CM5 sensor chip (GE Health) at about 1,200 resonance units. Proteins dialyzed in running buffer at 4°C were loaded onto the chip for 1 min, followed by injection of running buffer. A pulse of 5 μl of 10 mM NaOH and 1 M NaCl was injected to regenerate the surface.

Confocal Microscopy

ECs were fixed with PBS containing 3.7% paraformaldehyde, permeabilized with 0.1% Triton X-100 for 5 min, and stained with anti-Tβ4 (BioDesign, Saco, ME or Calbiochem, San Diego, CA), anti-ILK (Cell Signaling Technology, Danvers, MA), or anti-PFN-1 (Cell Signaling Technology) antibodies, followed by incubation with Alexa Fluor 488- or 568-conjugated IgG (Molecular Probes, Eugene, OR). For visualization of G-actin or F-actin, cells were labeled with Alexa Fluor 488- or 597-conjugated DNase I and Alexa Fluor 350-, 488-, or 568-phalloidin (Molecular Probes), respectively, and examined by confocal scanning using a TCS-SP microscope (Leica, Heidelberg, Germany). To avoid thickness artifacts, single-plane confocal images were obtained with a small, 1.0 Airy pinhole. Images were analyzed with ImagePro software (Media Cybernetics, Carlsbad, CA), and mean fluorescent intensity was quantified in 5–8 randomly selected 2 × 2 μM rectangles in each of 12 to 15 cells.

FRET

ECs were transfected with a plasmid encoding GFP-Linker^{GPVAT}-DsRed (as positive control), or cotransfected with plasmids expressing GFP and DsRed separately (as negative control) or plasmids expressing DsRed-tagged Tβ4 plus GFP-actin^{G13R}. Two FRET-based methods were used:

Acceptor Photobleaching ECs were fixed with 3.7% paraformaldehyde, and fluorescence images of fixed cells were taken in both donor (GFP) and acceptor (DsRed) channels before and after photobleaching. Acceptor photobleaching was performed with a 568 nm krypton laser at maximal power for a time

sufficient to provide 90% photobleaching. FRET efficiency was calculated as increased mean GFP fluorescence intensity in the photobleached area.

Sensitized Emission Transfected ECs were fixed and serial images acquired in three channels: GFP, DsRed, and FRET. Removal of spectral bleed-through, correction for differences in fluorophore expression levels, and background subtraction were performed with PFRET software (CircuSoft, Hockessin, DE). The results of FRET efficiency were displayed with a color spectrum.

FRAP

Molecular mobility of GFP-actin was evaluated by FRAP as described (Vasanji et al., 2004). In brief, ECs were transfected with pEGFP-actin and subjected to wound-induced migration. Medium was replaced with phenol red-free medium containing 25 mM HEPES. Living cells were photobleached in 2-μm-diameter circles using a 488 nm argon laser at maximal power. Recovery was monitored by repetitive scanning of bleached areas at 20% power. Fluorescence recovery curves were fit by nonlinear regression and expressed as lateral diffusion coefficients, *D*.

Plasmid-Based shRNA and Rescue

Duplex oligonucleotides encoding Tβ4 shRNA, PFN-1 shRNA, or control luciferase shRNA (Invitrogen) were annealed as a BamHI/HindIII fragment and cloned into pRNAT-U6-GFP/Neo (GenScript, Piscataway, NJ). Cells were transiently transfected with FuGene HD (Roche, Indianapolis, IN) and used 24 hr after transfection. Stably transfected EC lines were selected with 600 μg/ml neomycin, and colonies from a single cell maintained with 400 μg/ml neomycin. For Tβ4 reconstitution assay, stable Tβ4-depleted ECs were transfected with pcDNA (Vector), pcDNA-T$\beta4^{WT}$, pcDNA-T$\beta4^{K11P}$, or pcDNA-T$\beta4^{L17A}$ with FuGene HD overnight in medium containing 5% serum. For PFN rescue experiments, cells were transfected with pRNAT-Luc, or pRNAT-PFN-1 plus pcDNA (vector), pcDNA-Tβ4, or pcDNA-actin with or without mutations. Cells were cultured for another 24 hr and then replaced with serum-free medium for protease zymography, MMP-2 immunoblot assay, and wound-induced migration assay.

Statistical Analysis

Student's t test was used to calculate statistical significance with $p < 0.05$ representing a statistically significant difference.

Detailed methods for wound-induced cell migration assay, immunoprecipitation, immunoblot, optimization of FRET measurement, in vitro angiogenesis assay, siRNA treatment, MMP zymography, chemotaxis assay, protein pretreatment, and oligonucleotide primer sequences are in the Supplemental Experimental Procedures.

SUPPLEMENTAL DATA

Supplemental Data include Supplemental Experimental Procedures, one table, eleven figures, and one movie and can be found with this article online at http://www.developmentalcell.com/supplemental/S1534-5807(09)00130-0.

ACKNOWLEDGMENTS

We are grateful to Alan Levine, Tom Egelhoff, and Sanjay Pimplikar for helpful suggestions. We thank Amit Vasanji and Judith Drazba for technical assistance in image analysis. This work was supported by National Institutes of Health grants P01 HL29582, P01 HL76491, and R01 HL075255 (to P.L.F.) and by an American Heart Association Scientist Development Grant (to P.K.G.).

Received: May 11, 2008
Revised: February 4, 2009
Accepted: March 11, 2009
Published: May 18, 2009

REFERENCES

Ackah, E., Yu, J., Zoellner, S., Iwakiri, Y., Skurk, C., Shibata, R., Ouchi, N., Easton, R.M., Galasso, G., Birnbaum, M.J., et al. (2005). Akt1/protein kinase Bα is critical for ischemic and VEGF-mediated angiogenesis. J. Clin. Invest. *115*, 2119–2127.

Arboleda, M.J., Lyons, J.F., Kabbinavar, F.F., Bray, M.R., Snow, B.E., Ayala, R., Danino, M., Karlan, B.Y., and Slamon, D.J. (2003). Overexpression of AKT2/protein kinase Bbeta leads to up-regulation of β1 integrins, increased invasion, and metastasis of human breast and ovarian cancer cells. Cancer Res. *63*, 196–206.

Ballweber, E., Hannappel, E., Huff, T., Stephan, H., Haener, M., Taschner, N., Stoffler, D., Aebi, U., and Mannherz, H.G. (2002). Polymerisation of chemically cross-linked actin:thymosin beta(4) complex to filamentous actin: alteration in helical parameters and visualisation of thymosin beta(4) binding on F-actin. J. Mol. Biol. *315*, 613–625.

Bock-Marquette, I., Saxena, A., White, M.D., Dimaio, J.M., and Srivastava, D. (2004). Thymosin beta4 activates integrin-linked kinase and promotes cardiac cell migration, survival and cardiac repair. Nature *432*, 466–472.

Boudeau, J., Miranda-Saavedra, D., Barton, G.J., and Alessi, D.R. (2006). Emerging roles of pseudokinases. Trends Cell Biol. *16*, 443–452.

Buss, F., Temm-Grove, C., Henning, S., and Jockusch, B.M. (1992). Distribution of profilin in fibroblasts correlates with the presence of highly dynamic actin filaments. Cell Motil. Cytoskeleton *22*, 51–61.

Cao, L.G., Fishkind, D.J., and Wang, Y.L. (1993). Localization and dynamics of nonfilamentous actin in cultured cells. J. Cell Biol. *123*, 173–181.

Carlier, M.F., Didry, D., Erk, I., Lepault, J., Van Troys, M.L., Vandekerckhove, J., Perelroizen, I., Yin, H., Doi, Y., and Pantaloni, D. (1996). Tbeta 4 is not a simple G-actin sequestering protein and interacts with F-actin at high concentration. J. Biol. Chem. *271*, 9231–9239.

Cha, H.J., Jeong, M.J., and Kleinman, H.K. (2003). Role of thymosin β_4 in tumor metastasis and angiogenesis. J. Natl. Cancer Inst *95*, 1674–1680.

Chen, J., Somanath, P.R., Razorenova, O., Chen, W.S., Hay, N., Bornstein, P., and Byzova, T.V. (2005). Akt1 regulates pathological angiogenesis, vascular maturation and permeability in vivo. Nat. Med. *11*, 1188–1196.

Cheng, G.Z., Chan, J., Wang, Q., Zhang, W., Sun, C.D., and Wang, L.H. (2007). Twist transcriptionally up-regulates AKT2 in breast cancer cells leading to increased migration, invasion, and resistance to paclitaxel. Cancer Res. *67*, 1979–1987.

Cierniewski, C.S., Malinowski, M., Bednarek, R., and Cierniewska-Cieslak, A. (2007). Adhesive and proteolytic phenotype of migrating endothelial cells induced by thymosin beta-4. Ann. N Y Acad. Sci. *1112*, 123–139.

Cox, E.A., Sastry, S.K., and Huttenlocher, A. (2001). Integrin-mediated adhesion regulates cell polarity and membrane protrusion through the Rho family of GTPases. Mol. Biol. Cell *12*, 265–277.

Delcommenne, M., Tan, C., Gray, V., Rue, L., Woodgett, J., and Dedhar, S. (1998). Phosphoinositide-3-OH kinase-dependent regulation of glycogen synthase kinase 3 and protein kinase B/AKT by the integrin-linked kinase. Proc. Natl. Acad. Sci. USA *95*, 11211–11216.

Ding, Z., Lambrechts, A., Parepally, M., and Roy, P. (2006). Silencing profilin-1 inhibits endothelial cell proliferation, migration and cord morphogenesis. J. Cell Sci. *119*, 4127–4137.

Friedrich, E.B., Liu, E., Sinha, S., Cook, S., Milstone, D.S., MacRae, C.A., Mariotti, M., Kuhlencordt, P.J., Force, T., Rosenzweig, A., et al. (2004). Integrin-linked kinase regulates endothelial cell survival and vascular development. Mol. Cell. Biol. *24*, 8134–8144.

Ghosh, P.K., Vasanji, A., Murugesan, G., Eppell, S.J., Graham, L.M., and Fox, P.L. (2002). Membrane microviscosity regulates endothelial cell motility. Nat. Cell Biol. *4*, 894–900.

Giannone, G., Dubin-Thaler, B.J., Rossier, O., Cai, Y., Chaga, O., Jiang, G., Beaver, W., Dobereiner, H.G., Freund, Y., Borisy, G., and Sheetz, M.P. (2007). Lamellipodial actin mechanically links myosin activity with adhesion-site formation. Cell *128*, 561–575.

Goldstein, A.L., Hannappel, E., and Kleinman, H.K. (2005). Thymosin beta4: actin-sequestering protein moonlights to repair injured tissues. Trends Mol. Med. *11*, 421–429.

Gupton, S.L., and Waterman-Storer, C.M. (2006). Spatiotemporal feedback between actomyosin and focal-adhesion systems optimizes rapid cell migration. Cell *125*, 1361–1374.

Haas, T.L., and Madri, J.A. (1999). Extracellular matrix-driven matrix metalloproteinase production in endothelial cells: implications for angiogenesis. Trends Cardiovasc. Med. *9*, 70–77.

Huang, H.C., Hu, C.H., Tang, M.C., Wang, W.S., Chen, P.M., and Su, Y. (2007). Thymosin beta4 triggers an epithelial-mesenchymal transition in colorectal carcinoma by upregulating integrin-linked kinase. Oncogene *26*, 2781–2790.

Huff, T., Muller, C.S., Otto, A.M., Netzker, R., and Hannappel, E. (2001). beta-Thymosins, small acidic peptides with multiple functions. Int. J. Biochem. Cell Biol. *33*, 205–220.

Irie, H.Y., Pearline, R.V., Grueneberg, D., Hsia, M., Ravichandran, P., Kothari, N., Natesan, S., and Brugge, J.S. (2005). Distinct roles of Akt1 and Akt2 in regulating cell migration and epithelial-mesenchymal transition. J. Cell Biol. *171*, 1023–1034.

Irobi, E., Aguda, A.H., Larsson, M., Guerin, C., Yin, H.L., Burtnick, L.D., Blanchoin, L., and Robinson, R.C. (2004). Structural basis of actin sequestration by thymosin-beta4: implications for WH2 proteins. EMBO J. *23*, 3599–3608.

Joshi, M.B., Ivanov, D., Philippova, M., Erne, P., and Resink, T.J. (2007). Integrin-linked kinase is an essential mediator for T-cadherin-dependent signaling via Akt and GSK3beta in endothelial cells. FASEB J. *21*, 3083–3095.

Kobayashi, T., Okada, F., Fujii, N., Tomita, N., Ito, S., Tazawa, H., Aoyama, T., Choi, S.K., Shibata, T., Fujita, H., and Hosokawa, M. (2002). Thymosin-beta4 regulates motility and metastasis of malignant mouse fibrosarcoma cells. Am. J. Pathol. *160*, 869–882.

Lauffenburger, D.A., and Horwitz, A.F. (1996). Cell migration: a physically integrated molecular process. Cell *84*, 359–369.

Li, Y., Yang, J., Dai, C., Wu, C., and Liu, Y. (2003). Role for integrin-linked kinase in mediating tubular epithelial to mesenchymal transition and renal interstitial fibrogenesis. J. Clin. Invest *112*, 503–516.

Malik, M.T., and Kakar, S.S. (2006). Regulation of angiogenesis and invasion by human Pituitary tumor transforming gene (PTTG) through increased expression and secretion of matrix metalloproteinase-2 (MMP-2). Mol. Cancer *5*, 61.

Malinda, K.M., Goldstein, A.L., and Kleinman, H.K. (1997). Thymosin beta 4 stimulates directional migration of human umbilical vein endothelial cells. FASEB J. *11*, 474–481.

McDonald, D., Carrero, G., Andrin, C., de Vries, G., and Hendzel, M.J. (2006). Nucleoplasmic beta-actin exists in a dynamic equilibrium between low-mobility polymeric species and rapidly diffusing populations. J. Cell Biol. *172*, 541–552.

McGrath, J.L., Hartwig, J.H., Tardy, Y., and Dewey, C.F., Jr. (1998). Measuring actin dynamics in endothelial cells. Microsc. Res. Tech. *43*, 385–394.

Pantaloni, D., and Carlier, M.F. (1993). How profilin promotes actin filament assembly in the presence of thymosin β4. Cell *75*, 1007–1014.

Philp, D., Huff, T., Gho, Y.S., Hannappel, E., and Kleinman, H.K. (2003). The actin binding site on thymosin beta4 promotes angiogenesis. FASEB J. *17*, 2103–2105.

Philp, D., Scheremeta, B., Sibliss, K., Zhou, M., Fine, E.L., Nguyen, M., Wahl, L., Hoffman, M.P., and Kleinman, H.K. (2006). Thymosin beta4 promotes matrix metalloproteinase expression during wound repair. J. Cell. Physiol. *208*, 195–200.

Phung, T.L., Ziv, K., Dabydeen, D., Eyiah-Mensah, G., Riveros, M., Perruzzi, C., Sun, J., Monahan-Earley, R.A., Shiojima, I., Nagy, J.A., et al. (2006). Pathological angiogenesis is induced by sustained Akt signaling and inhibited by rapamycin. Cancer Cell *10*, 159–170.

Pollard, T.D., Blanchoin, L., and Mullins, R.D. (2000). Molecular mechanisms controlling actin filament dynamics in nonmuscle cells. Annu. Rev. Biophys. Biomol. Struct. *29*, 545–576.

Pollard, T.D., and Borisy, G.G. (2003). Cellular motility driven by assembly and disassembly of actin filaments. Cell *112*, 453–465.

Posern, G., Sotiropoulos, A., and Treisman, R. (2002). Mutant actins demonstrate a role for unpolymerized actin in control of transcription by serum response factor. Mol. Biol. Cell *13*, 4167–4178.

Qiu, P., Kurpakus-Wheater, M., and Sosne, G. (2007). Matrix metalloproteinase activity is necessary for thymosin beta 4 promotion of epithelial cell migration. J. Cell. Physiol. *212*, 165–173.

Ren, X.D., Kiosses, W.B., and Schwartz, M.A. (1999). Regulation of the small GTP-binding protein Rho by cell adhesion and the cytoskeleton. EMBO J. *18*, 578–585.

Ridley, A.J., Schwartz, M.A., Burridge, K., Firtel, R.A., Ginsberg, M.H., Borisy, G., Parsons, J.T., and Horwitz, A.R. (2003). Cell migration: integrating signals from front to back. Science *302*, 1704–1709.

Safer, D., Elzinga, M., and Nachmias, V.T. (1991). Thymosin beta 4 and Fx, an actin-sequestering peptide, are indistinguishable. J. Biol. Chem. *266*, 4029–4032.

Safer, D., Sosnick, T.R., and Elzinga, M. (1997). Thymosin beta 4 binds actin in an extended conformation and contacts both the barbed and pointed ends. Biochemistry *36*, 5806–5816.

Sanders, M.C., Goldstein, A.L., and Wang, Y.L. (1992). Thymosin beta 4 (Fx peptide) is a potent regulator of actin polymerization in living cells. Proc. Natl. Acad. Sci. USA *89*, 4678–4682.

Sithanandam, G., Fornwald, L.W., Fields, J., and Anderson, L.M. (2005). Inactivation of ErbB3 by siRNA promotes apoptosis and attenuates growth and invasiveness of human lung adenocarcinoma cell line A549. Oncogene *24*, 1847–1859.

Smart, N., Risebro, C.A., Melville, A.A., Moses, K., Schwartz, R.J., Chien, K.R., and Riley, P.R. (2007). Thymosin beta4 induces adult epicardial progenitor mobilization and neovascularization. Nature *445*, 177–182.

Tan, C., Cruet-Hennequart, S., Troussard, A., Fazli, L., Costello, P., Sutton, K., Wheeler, J., Gleave, M., Sanghera, J., and Dedhar, S. (2004). Regulation of tumor angiogenesis by integrin-linked kinase (ILK). Cancer Cell *5*, 79–90.

Troussard, A.A., Mawji, N.M., Ong, C., Mui, A., St-Arnaud, R., and Dedhar, S. (2003). Conditional knock-out of integrin-linked kinase demonstrates an essential role in protein kinase B/Akt activation. J. Biol. Chem. *278*, 22374–22378.

Van Troys, M., Dewitte, D., Goethals, M., Carlier, M.F., Vandekerckhove, J., and Ampe, C. (1996). The actin binding site of thymosin β_4 mapped by mutational analysis. EMBO J. *15*, 201–210.

Vasanji, A., Ghosh, P.K., Graham, L.M., Eppell, S.J., and Fox, P.L. (2004). Polarization of plasma membrane microviscosity during endothelial cell migration. Dev. Cell *6*, 29–41.

Vouret-Craviari, V., Boulter, E., Grall, D., Matthews, C., and Van Obberghen-Schilling, E. (2004). ILK is required for the assembly of matrix-forming adhesions and capillary morphogenesis in endothelial cells. J. Cell Sci. *117*, 4559–4569.

White, D.E., Coutu, P., Shi, Y.F., Tardif, J.C., Nattel, S., St Arnaud, R., Dedhar, S., and Muller, W.J. (2006). Targeted ablation of ILK from the murine heart results in dilated cardiomyopathy and spontaneous heart failure. Genes Dev. *20*, 2355–2360.

Witke, W. (2004). The role of profilin complexes in cell motility and other cellular processes. Trends Cell Biol. *14*, 461–469.

Wu, C., and Dedhar, S. (2001). Integrin-linked kinase (ILK) and its interactors: a new paradigm for the coupling of extracellular matrix to actin cytoskeleton and signaling complexes. J. Cell Biol. *155*, 505–510.

Yu, F.X., Lin, S.C., Morrison-Bogorad, M., Atkinson, M.A., and Yin, H.L. (1993). Thymosin beta 10 and thymosin beta 4 are both actin monomer sequestering proteins. J. Biol. Chem. *268*, 502–509.

Zhou, G.L., Tucker, D.F., Bae, S.S., Bhatheja, K., Birnbaum, M.J., and Field, J. (2006). Opposing roles for Akt1 and Akt2 in Rac/Pak signaling and cell migration. J. Biol. Chem. *281*, 36443–36453.